# Supplementary Information

# Construction of uniform Ziolitic imidazole framework (ZIF-8) nanocrystal through wet chemical route: towards the supercapacitor application

Iqra Rabani[a*], Je-Won Lee[a], Taeyoon Lim[a], Hai Bang Truong[b,c], Sobia Nisar[d], Sitara Afzal[e], and Young-Soo Seo[a*]

[a]Department of Nanotechnology and Advanced Materials Engineering, Sejong University, Seoul 05006, Republic of Korea

[b]Optical Materials Research Group, Science and Technology Advanced Institute, Van Lang University, Ho Chi Minh City, Viet Nam (truonghaibang@vlu.edu.vn)

[c]Faculty of Applied Technology, School of Engineering and Technology, Van Lang University, Ho Chi Minh City, Viet Nam

[d]Department of electronic engineering, Sejong University, Seoul 05006, Republic of Korea

[e]Mixed reality and interaction laboratory, Sejong University, Seoul 05006, Republic of Korea

*Equivalent Corresponding author's e-mail: iqrarabani@sejong.ac.kr & ysseo@sejong.ac.kr

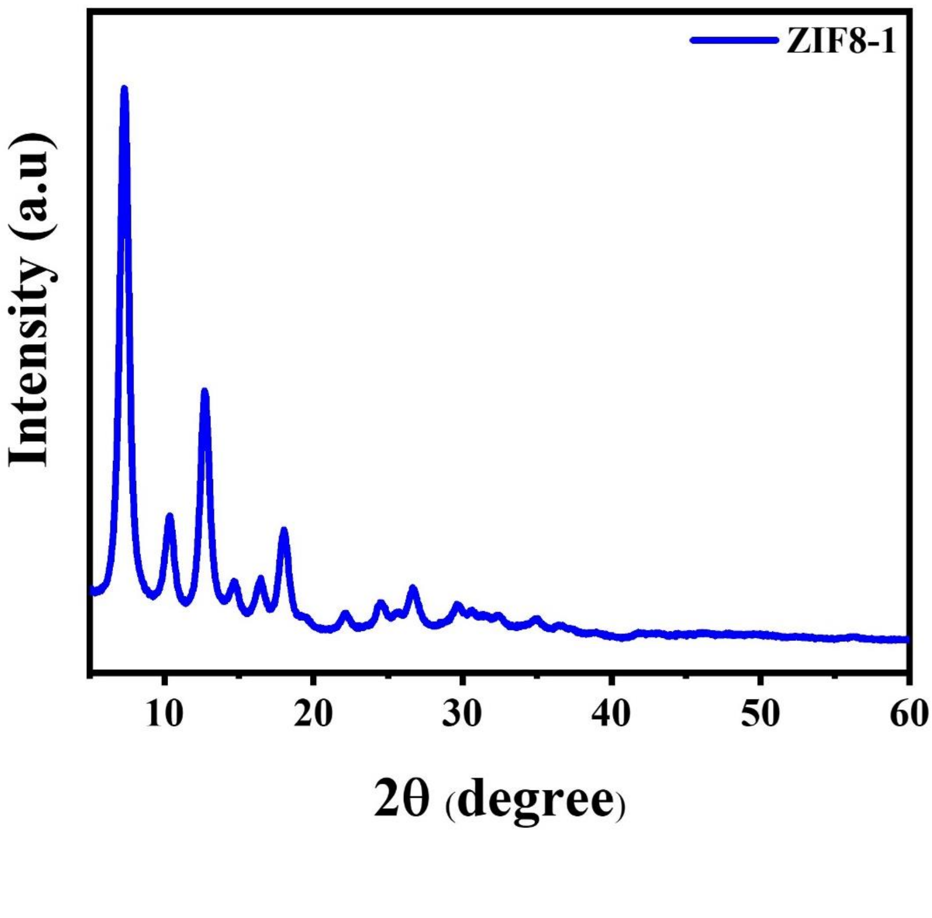


***Figure S1:*** *XRD pattern of the ZIF8-1 nanocrystals.*

***Table S1***. *Raman Band assignments for ZIF8 nanocrystals. .*

| ***Frequency (cm $^{-1}$)*** | ***Band Assignments[a]*** |
|---|---|
| *273* | *v Zn-N* |
| *686* | *Imidazole ring puckering* |
| *833* | *C-H oop bend (C4-C5)* |
| *1021* | *C-H oop bend* |
| *1146* | *v C5-N* |
| *1187* | *v C-N+N-H wag* |
| *1311* | *Ring expansion+N-H wag* |
| *1385* | *CH3 bending* |
| *1460* | *C-H wag* |
| *1508* | *v C4-C5* |
| *2930* | $v_{asym}$ *C-H (methyl)* |
| *3131* | *v C-H (ar)* |

[a] ν: stretching, oop: out of plane, ar: aromatic, asym: asymmetric.

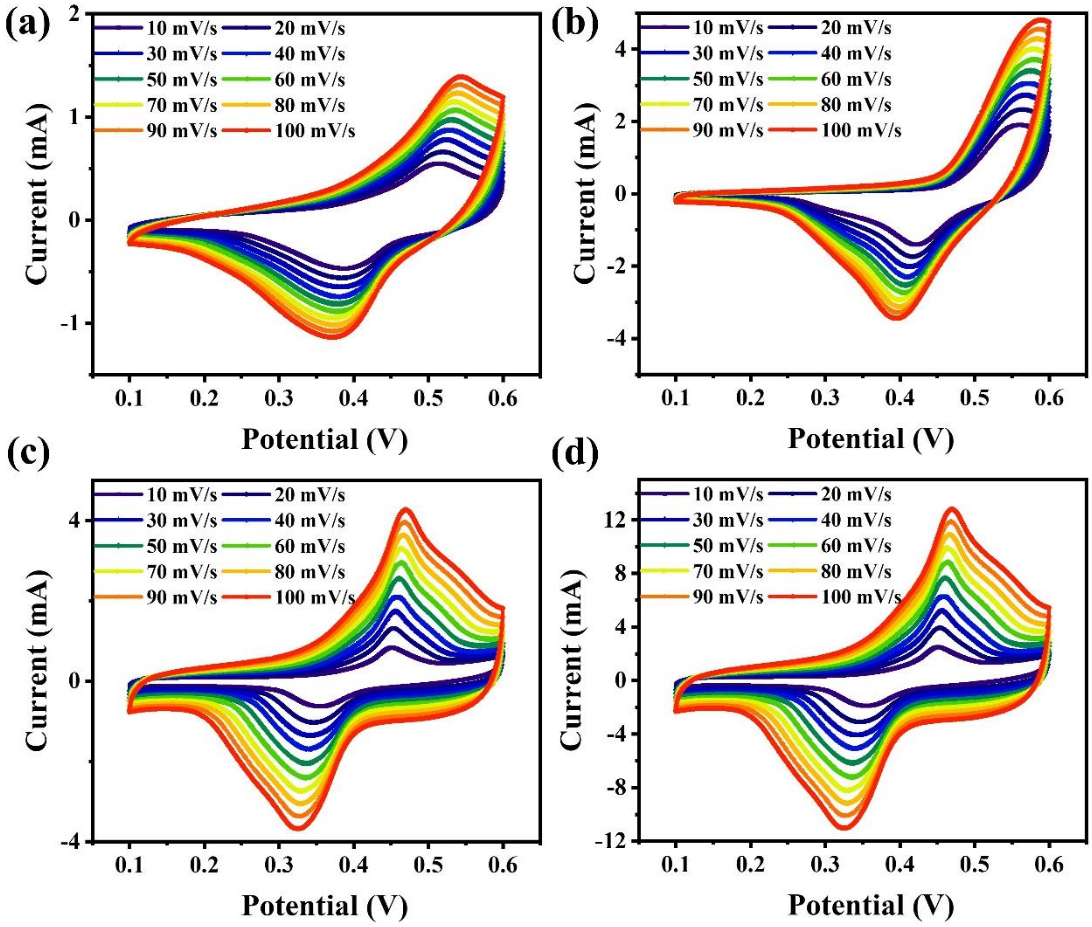


***Figure S2:*** *Cyclic voltametric (CV) profiles using 0.5 M* $H_2SO_4$ *at various scan rates for* ***(a)*** *ZIF8-1nanocrsytal electrode,* ***(b)*** *ZIF8-2 nanocrystal electrode,* ***(c)*** *ZIF8-3 nanocrystal electrode and* ***(d)*** *ZIF8-4 nanocrystal electrode, respectively.*

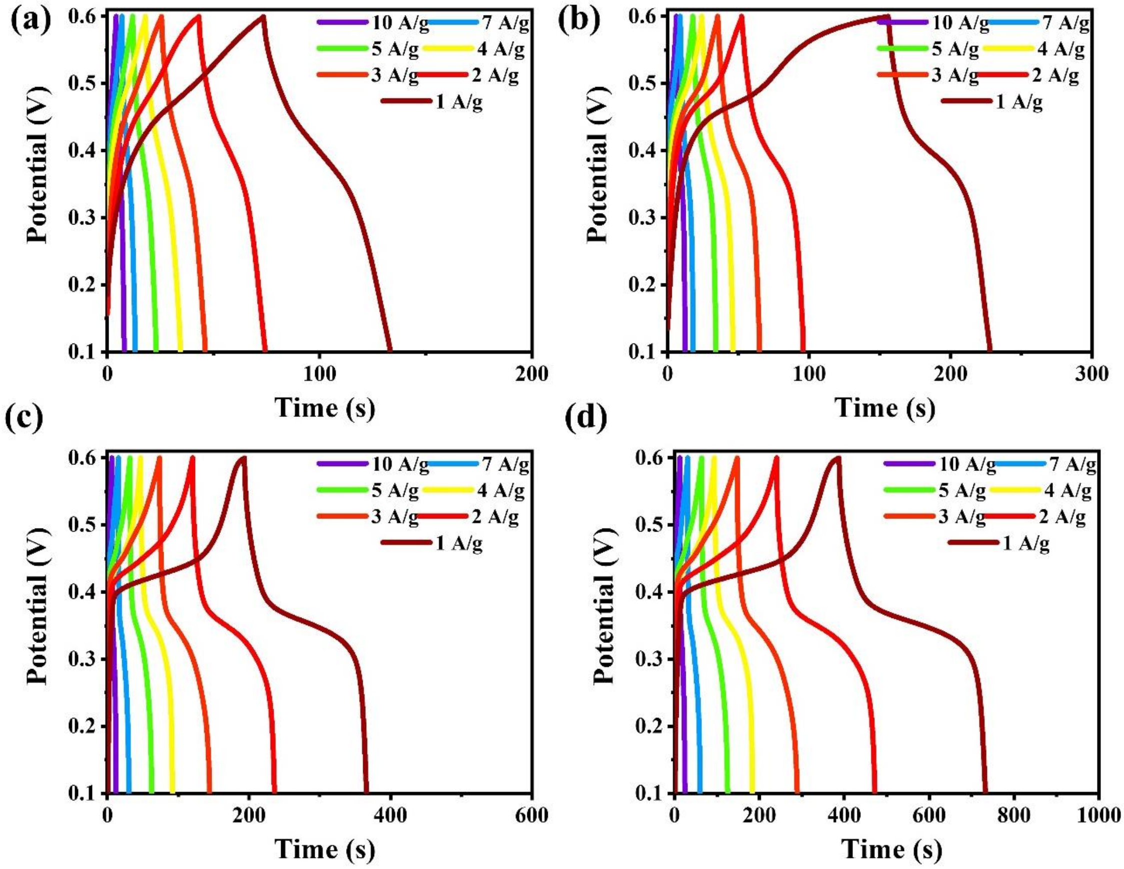


***Figure S3:*** *Galvanostatic charging-discharging (GCD) profiles using 0.5 M $H_2SO_4$ at various current densities for **(a)** ZIF8-1nanocrsytal electrode, **(b)** ZIF8-2 nanocrystal electrode, **(c)** ZIF8-3 nanocrystal electrode and **(d)** ZIF8-4 nanocrystal electrode, respectively.*

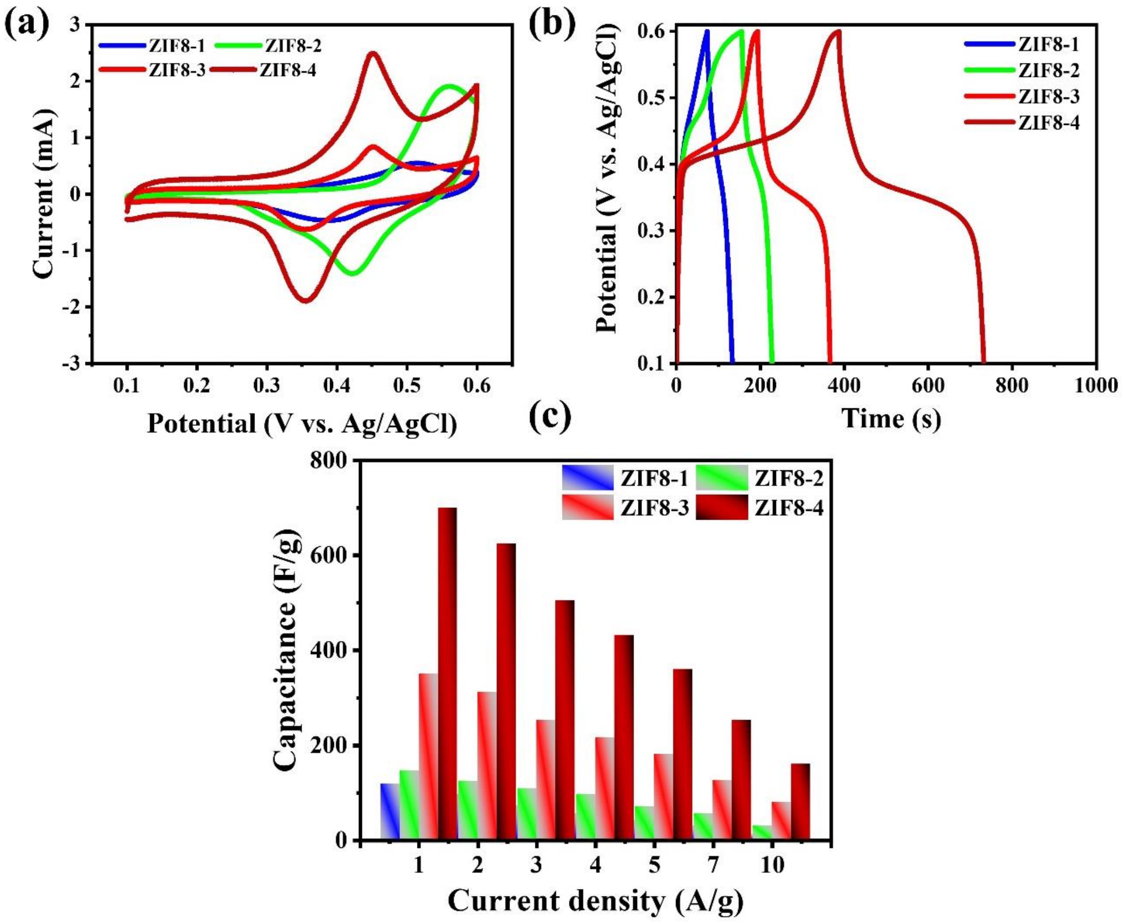


***Figure S4:*** *Electrochemical performance using 0.5 M* $H_2SO_4$*;* ***(a)*** *comparative CV profiles for the ZIF8-1, ZIF8-2, ZIF8-3, ZIF8-4 nanocrystal electrodes at fixed scan rate of 10 mV/s,* ***(b)*** *comparative GCD profiles for the ZIF8-1, ZIF8-2, ZIF8-3, ZIF8-4 nanocrystal electrodes at fixed current density of 1 A/g and* ***(c)*** *specific capacitance against current densities.*

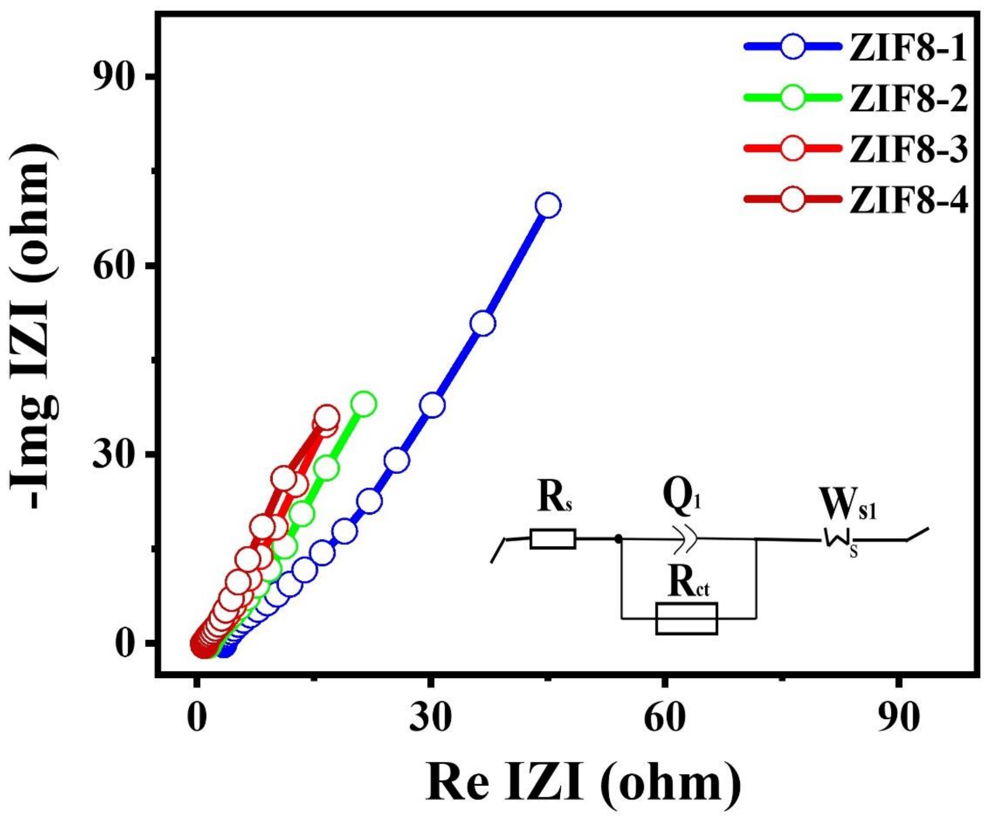


***Figure S5:*** *Nyquist plot with equivalent fitted circuit for the ZIF8-1, ZIF8-2, ZIF8-3 and ZIF8-4 nanocrystals.*

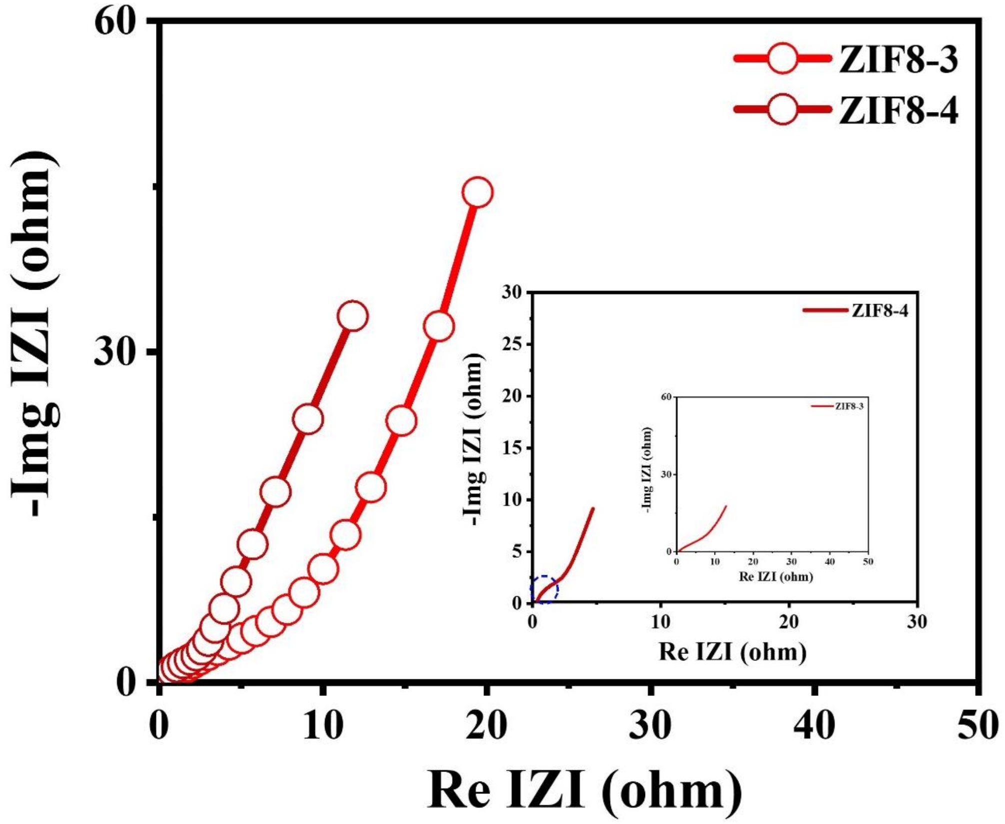


***Figure S6:*** *Nyquist plot with equivalent fitted circuit for the ZIF8-3 and ZIF8-4 SSCs.*

**Table S2.** Comparison of electrochemical performance of the ZIF's based materials reported to date with those in the present study in three electrode measurement.

| Electrode Material | Electrolyte | Specific Capacitance ($F.g^{-1}$) | Current Density ($A.g^{-1}$) | Ref |
|---|---|---|---|---|
| **ZIF8-4** | **1 M KOH** | **1420** | **1** | **This work** |
| **ZIF8-3** | **1 M KOH** | **693** | **1** | |
| **ZIF8-2** | **1 M KOH** | **545** | **1** | |
| **ZIF8-1** | **1 M KOH** | **344** | **1** | |
| **ZIF-67-PPy-2** | 1 M $Na_2SO_4$ | 554 | 0.5 | [1] |
| **ZIF-67/PPy** | --- | 1241 | 1 | [2] |
| **rGO/RuO** | $Na_2SO_4$ | --- | --- | [3] |
| **RuO** | $Na_2SO_4$ | --- | --- | [3] |
| **ZIF-69@Activated Carbon** | 0.5 M $H_2SO_4$ | 168 F | --- | [4] |
| **ZIF-8@Nanoporous carbon** | 1 M $H_2SO_4$ | 251 | --- | [5] |
| **ZIF-8@Carbon nanofiber** | 1 M $H_2SO_4$ | 322 | 1 | [6] |
| **ZIF-8/GO** | 1 M $H_2SO_4$ | 238 | 1 | [7] |
| **ZIF-8/67** | 0.5 M $H_2SO_4$ | 286 | 2.5 | [8] |
| **ZIF-8/MWCNT** | 1 M $H_2SO_4$ | 326 | 1 | [9] |
| **ZIF-7/glucose** | 6 M KOH | 228 | 0.1 | [10] |
| **ZIF-67@BIC carbon** | 1 M KOH | 119 | 0.5 | [11] |
| **ZIF-8@hollow carbon spheres** | 6 M KOH | 280 | 1 | [12] |
| **ZIF-8@porous carbon** | 1 M KOH | 1370 | 1 | [13] |
| **rGO/$RuO_2$** | 3 M $H_2SO_4$ | 321.5 | 0.5 | [14] |
| **$RuO_2$/Graphene** | 1 M $Na_2SO_4$ | 441.1 | 0.1 | [15] |
| **$RuO_2$ NRs/C** | 1 M $H_2SO_4$ | 151. 1 | 5 | [16] |
| **$RuO_2$/GC** | 2 M $H_2SO_4$ | 422.4 | 0.6 | [17] |

| | | | | |
|---|---|---|---|---|
| **ZnO-NiO** | --- | 4.1 | 5 | [18] |
| **ZnO nanocones** | --- | 378.5 | 1 | [19] |
| **$ZnMoO_4$/CoO** | --- | 4.47 | 2 | [20] |
| **ZnO/$MnO_2$ nanowires** | 1 M $Na_2SO_4$ | 501 | 2 | [21] |
| **$ZnMn_2O_4$/carbon** | 6 M KOH | 105 | 0.3 | [22] |
| **ZnO nanocones** | 1 M KOH | 236 | 1 | [23] |
| **NCA/$Co_3O_4$** | 6 M KOH | 616 | 1.2 | [24] |
| **ZnO/$MnO_2$** | 0.5 M $Na_2SO_4$ | 262 | 0.2 | [25] |
| **ZnO/MnO nanoflowers** | 1 M $Na_2SO_4$ | 556 | 1 | [26] |
| **ZnO-/core like $MnO_2$** | 1 M $Na_2SO_4$ | 221 | 0.5 | [27] |
| **ZnO/$MnO_2$ core/shell** | 1 M $Na_2SO_4$ | 424 | 0.5 | [28] |
| **$RuO_2$** | --- | 648 | --- | [29] |
| **Annealed RGO-$RuO_2$** | 1 M $H_2SO_4$ | 509.4 | 1.20 | [30] |
| **h$RuO_2$/C** | 1 M $H_2SO_4$ | 516.4<br>507.2<br>495.0 | 0.2<br>0.5<br>1 | [31] |
| **h$RuO_2$/CNT** | 1 M $H_2SO_4$ | 474.7<br>444.6<br>403.7 | 0.2<br>0.5<br>1 | [31] |
| **Commercial $RuO_2$/C** | 1 M $H_2SO_4$ | 402.7<br>360.5<br>332.2 | 0.2<br>0.5<br>1 | [31] |
| **Hydrous $RuO_2$/Ketjen black** | 0.5 M $H_2SO_4$ | 647 | --- | [32] |
| **Carbon-Ru xerogel** | --- | 256 | 0.1 | [33] |

| | | | | |
|---|---|---|---|---|
| **$RuO_2/MnO_2$** | --- | 438 | --- | [34] |
| **$RuO_2/TiO_2$** | PVA-$H_3PO_4$-$H_2O$ | 229.9 | 0.7 | [35] |
| **RuOsOx/G** | 1 M $H_2SO_4$ | 729 | 1 | [36] |

**References**

[1] X. Xu, J. Tang, H. Qian, S. Hou, Y. Bando, M.S.A. Hossain, L. Pan, Y. Yamauchi, Three-dimensional networked metal–organic frameworks with conductive polypyrrole tubes for flexible supercapacitors, ACS applied materials & interfaces, 9 (2017) 38737-38744.

[2] Y. Han, C. Liu, W. Yue, A. Huang, One-pot synthesis of conductive polypyrrole incorporated ZIF-67 for high-performance supercapacitors, Materials Letters, 318 (2022) 132158.

[3] V.U. Shankar, P.S. Kumar, D. Govindarajan, P. Nethaji, G.B. Balji, Ruthenium dioxide anchored on reduced graphene oxide nanocomposite for 1.2 V symmetric supercapacitor devices, Sustainable Energy Technologies and Assessments, 53 (2022) 102444.

[4] Q. Wang, W. Xia, W. Guo, L. An, D. Xia, R. Zou, Functional zeolitic-imidazolate-framework-templated porous carbon materials for CO2 capture and enhanced capacitors, Chemistry–An Asian Journal, 8 (2013) 1879-1885.

[5] R.R. Salunkhe, Y. Kamachi, N.L. Torad, S.M. Hwang, Z. Sun, S.X. Dou, J.H. Kim, Y. Yamauchi, Fabrication of symmetric supercapacitors based on MOF-derived nanoporous carbons, Journal of Materials Chemistry A, 2 (2014) 19848-19854.

[6] C. Wang, C. Liu, J. Li, X. Sun, J. Shen, W. Han, L. Wang, Electrospun metal–organic framework derived hierarchical carbon nanofibers with high

performance for supercapacitors, Chemical Communications, 53 (2017) 1751-1754.

[7] C. Li, C. Hu, Y. Zhao, L. Song, J. Zhang, R. Huang, L. Qu, Decoration of graphene network with metal–organic frameworks for enhanced electrochemical capacitive behavior, Carbon, 78 (2014) 231-242.

[8] J. Kim, C. Young, J. Lee, M.-S. Park, M. Shahabuddin, Y. Yamauchi, J.H. Kim, CNTs grown on nanoporous carbon from zeolitic imidazolate frameworks for supercapacitors, Chemical Communications, 52 (2016) 13016-13019.

[9] Y. Wang, B. Chen, Y. Zhang, L. Fu, Y. Zhu, L. Zhang, Y. Wu, ZIF-8@ MWCNT-derived carbon composite as electrode of high performance for supercapacitor, Electrochimica Acta, 213 (2016) 260-269.

[10] P. Zhang, F. Sun, Z. Shen, D. Cao, ZIF-derived porous carbon: a promising supercapacitor electrode material, Journal of Materials Chemistry A, 2 (2014) 12873-12880.

[11] X. Deng, S. Zhu, J. Li, L. Ma, F. He, E. Liu, C. He, C. Shi, Q. Li, N. Zhao, Ball-in-cage nanocomposites of metal–organic frameworks and three-dimensional carbon networks: synthesis and capacitive performance, Nanoscale, 9 (2017) 6478-6485.

[12] L. Xin, R. Chen, Q. Liu, J. Liu, Z. Li, R. Li, J. Wang, Composites of hierarchical metal–organic framework derived nitrogen-doped porous carbon and

interpenetrating 3D hollow carbon spheres from lotus pollen for high-performance supercapacitors, New Journal of Chemistry, 41 (2017) 12835-12842.

[13] B. Han, G. Cheng, E. Zhang, L. Zhang, X. Wang, Three dimensional hierarchically porous ZIF-8 derived carbon/LDH core-shell composite for high performance supercapacitors, Electrochimica Acta, 263 (2018) 391-399.

[14] S. Korkmaz, İ.A. Kariper, O. Karaman, C. Karaman, The production of rGO/RuO2 aerogel supercapacitor and analysis of its electrochemical performances, Ceramics International, 47 (2021) 34514-34520.

[15] R. Thangappan, M. Arivanandhan, R.D. Kumar, R. Jayavel, Facile synthesis of RuO2 nanoparticles anchored on graphene nanosheets for high performance composite electrode for supercapacitor applications, Journal of Physics and Chemistry of Solids, 121 (2018) 339-349.

[16] T.N.J.I. Edison, R. Atchudan, Y.R. Lee, Facile synthesis of carbon encapsulated RuO2 nanorods for supercapacitor and electrocatalytic hydrogen evolution reaction, International Journal of Hydrogen Energy, 44 (2019) 2323-2329.

[17] S. Kong, K. Cheng, T. Ouyang, Y. Gao, K. Ye, G. Wang, D. Cao, Facile electrodepositing processed of RuO2-graphene nanosheets-CNT composites as a binder-free electrode for electrochemical supercapacitors, Electrochimica Acta, 246 (2017) 433-442.

[18] X. Zheng, X. Yan, Y. Sun, Z. Bai, G. Zhang, Y. Shen, Q. Liang, Y. Zhang, Au-embedded ZnO/NiO hybrid with excellent electrochemical performance as

advanced electrode materials for supercapacitor, ACS applied materials & interfaces, 7 (2015) 2480-2485.

[19] S.S. Karade, B.R. Sankapal, Two dimensional cryptomelane like growth of MoSe2 over MWCNTs: symmetric all-solid-state supercapacitor, Journal of Electroanalytical Chemistry, 802 (2017) 131-138.

[20] P. Li, C. Ruan, J. Xu, Y. Xie, A high-performance asymmetric supercapacitor electrode based on a three-dimensional ZnMoO 4/CoO nanohybrid on nickel foam, Nanoscale, 11 (2019) 13639-13649.

[21] S. Li, J. Wen, X. Mo, H. Long, H. Wang, J. Wang, G. Fang, Three-dimensional MnO2 nanowire/ZnO nanorod arrays hybrid nanostructure for high-performance and flexible supercapacitor electrode, Journal of Power Sources, 256 (2014) 206-211.

[22] C.-K. Sim, S.R. Majid, N.Z. Mahmood, Durable porous carbon/ZnMn2O4 composite electrode material for supercapacitor, Journal of Alloys and Compounds, 803 (2019) 424-433.

[23] X. He, J.E. Yoo, M.H. Lee, J. Bae, Morphology engineering of ZnO nanostructures for high performance supercapacitors: enhanced electrochemistry of ZnO nanocones compared to ZnO nanowires, Nanotechnology, 28 (2017) 245402.

[24] G. Sun, L. Ma, J. Ran, X. Shen, H. Tong, Incorporation of homogeneous Co 3 O 4 into a nitrogen-doped carbon aerogel via a facile in situ synthesis method:

implications for high performance asymmetric supercapacitors, Journal of Materials Chemistry A, 4 (2016) 9542-9554.

[25] W. Li, G. He, J. Shao, Q. Liu, K. Xu, J. Hu, I.P. Parkin, Urchin-like MnO2 capped ZnO nanorods as high-rate and high-stability pseudocapacitor electrodes, Electrochimica Acta, 186 (2015) 1-6.

[26] E. Samuel, B. Joshi, Y.-i. Kim, A. Aldalbahi, M. Rahaman, S.S. Yoon, ZnO/MnO x nanoflowers for high-performance supercapacitor electrodes, ACS Sustainable Chemistry & Engineering, 8 (2020) 3697-3708.

[27] Y. Zhao, P. Jiang, S.-S. Xie, ZnO-template-mediated synthesis of three-dimensional coral-like MnO2 nanostructure for supercapacitors, Journal of power sources, 239 (2013) 393-398.

[28] M. Huang, F. Li, X.L. Zhao, D. Luo, X.Q. You, Y.X. Zhang, G. Li, Hierarchical ZnO@ MnO2 core-shell pillar arrays on Ni foam for binder-free supercapacitor electrodes, Electrochimica Acta, 152 (2015) 172-177.

[29] R.-R. Bi, X.-L. Wu, F.-F. Cao, L.-Y. Jiang, Y.-G. Guo, L.-J. Wan, Highly dispersed RuO2 nanoparticles on carbon nanotubes: facile synthesis and enhanced supercapacitance performance, The Journal of Physical Chemistry C, 114 (2010) 2448-2451.

[30] F. Amir, V. Pham, J. Dickerson, Facile synthesis of ultra-small ruthenium oxide nanoparticles anchored on reduced graphene oxide nanosheets for high-performance supercapacitors, RSC Advances, 5 (2015) 67638-67645.

[31] P. Wang, Y. Xu, H. Liu, Y. Chen, J. Yang, Q. Tan, Carbon/carbon nanotube-supported RuO2 nanoparticles with a hollow interior as excellent electrode materials for supercapacitors, Nano Energy, 15 (2015) 116-124.

[32] M. Min, K. Machida, J.H. Jang, K. Naoi, Hydrous RuO2/carbon black nanocomposites with 3D porous structure by novel incipient wetness method for supercapacitors, Journal of the Electrochemical Society, 153 (2005) A334.

[33] C. Lin, J.A. Ritter, B.N. Popov, Development of Carbon-Metal Oxide Supercapacitors from Sol-Gel Derived Carbon-Ruthenium Xerogels, Journal of the Electrochemical Society, 146 (1999) 3155.

[34] J. Lei, X. Chen, RuO2/MnO2 composite materials for high-performance supercapacitor electrodes, Journal of Semiconductors, 36 (2015) 083006.

[35] W. Yong-gang, Z. Xiao-gang, Preparation and electrochemical capacitance of RuO2/TiO2 nanotubes composites, Electrochimica Acta, 49 (2004) 1957-1962.

[36] M. Sarno, E. Ponticorvo, D. Scarpa, Ru and Os based new electrode for electrochemical flow supercapacitors, Chem Eng J, 377 (2019) 120050.